Plasma Sources Sci. Technol. 4 (1995) 511–515. Printed in the UK

Characterization of a laser-ablation-assisted-plasma-discharge-metallic ion source

J S Lash, R M Gilgenbach† and H L Spindler

Intense Energy Beam Interaction Laboratory, Department of Nuclear Engineering, The University of Michigan, Ann Arbor, MI 48109–2104, USA

Received 3 January 1995, in final form 2 August 1995

Abstract. Experiments have been carried out to characterize further the properties of a new laser-ablation-assisted-plasma-discharge source of metallic aluminium ions. Laser ablation is accomplished by focusing a KrF excimer laser (< 1.2 J, 40 ns, 248 nm) onto a solid aluminium target with a fluence of approximately 10 J cm^{-2}. Through gated optical emission spectroscopy, the laser ablation plume optical emission is observed to contain only aluminium neutral atom transitions after approximately 100 ns. With the application of a 3.6 kV, 760 A discharge, the neutral atom plume is transformed into a plasma with the emission dominated by Al^{+} and Al^{2+} ion transitions. Through time-resolved spectroscopy, emission intensity from the Al neutral species and the Al^{2+} ion species is observed to coincide with current peaks through the plasma. Spectroscopic measurements indicate an Al^{2+} electronic temperature of 3 eV (and an Al^{+} electronic temperature of 1 eV) which, since local thermodynamic equilibrium (LTE) is applicable for the observed emission, provide a free electron temperature of 1 to 3 eV. A simple LTE model suggests an electron temperature of 1.2 eV for equal Al^{+} and Al^{2+} ion fractions. A floating double Langmuir probe measurement 1 mm in front of the laser ablation spot indicates an electron temperature of roughly 1 eV and an ion density of approximately 5×10^{14} cm^{-3} during the second current lobe.

1. Introduction

In recent years many new electronic materials which depend on the deposition and implantation of metallic and high-mass elements onto various types of substrates have been developed. Hence, there is a need for an ion source capable of producing ions of any element in the periodic table as well as being able to deposit the source material on a given substrate. Laser ablation has been widely used to ablate material to produce thin films of metals [1], metal-nitrides [2], and metal-oxides [3]. However neutral–metal atom density measurements and spectroscopic measurements suggest the fractional ionization is relatively low in laser ablation plumes from metals at low fluences [4–7]. Other researchers have found that by applying a magnetic field transverse to the plume flow, ionization has been enhanced in the ablation of MgO by hindering the recombination of the initial plasma [8]. In the experiments reported here, laser-ablation-assisted-plasma-discharges (LAAPDs) are produced by a high-voltage (1.4–3.6 kV) and high-current (280–760 A) electrical discharge through the plume. The high discharge power (~MW) supplied by a pulsed capacitor bank is sufficient to generate a nearly fully ionized plume of metal ions from the laser ablated aluminium target. This source is advantageous since, in theory, ions can be created from any material that can be ablated with a laser.

An important application of the discharge plasma is its use in thin film deposition. With the ability to increase the ionization fraction in the laser ablation plume significantly, the effect of ions on film quality can also be studied. It is well known that large particulate is generated in laser ablation [9]. Possibly this discharge can be used to disintegrate the particulate and create a nearly atomic or ionic plume. A number of other researchers have employed the voltage between the target and substrate to stimulate and enhance film deposition, but with only a qualitative analysis [10–12]. Here we present a further characterization of a LAAPD ion source [13]. Time-resolved optical emission spectroscopy has been used to determine the species evolution and relate this to the discharge parameters. Spectroscopic measurements have been used to determine the electronic temperature of the ion species, while a floating double Langmuir probe has measured the electron temperature, as well as the ion density.

† To whom all correspondence should be addressed.

0963-0252/95/040511+05$19.50

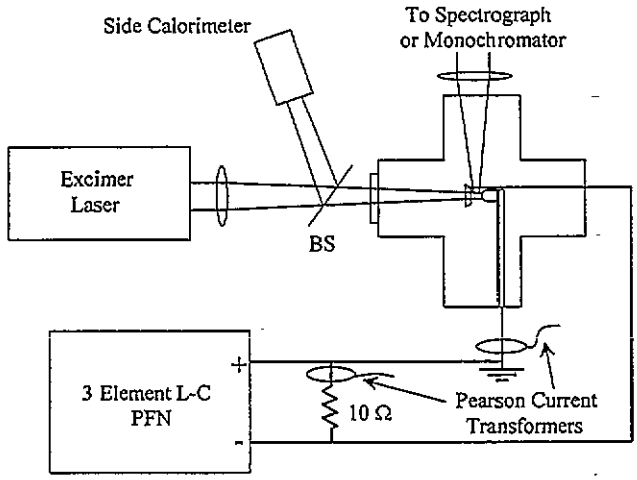

Figure 1. Simplified laser-ablation-assisted-plasma discharge experimental configuration.

2. Experimental configuration

Figure 1 shows the simplified LAAPD experimental configuration. Laser ablation plumes are generated by focusing a Lumonics TE-292K KrF excimer laser (< 1.2 J, 40 ns, 248 nm) with a $f = 25$ cm lens onto a solid aluminium target (99.999%). The focused laser spot size is 0.05 cm^2, as determined by measuring the region of surface modification, yielding a fluence of ~ 10 J cm^{-2}. The incident laser energy is monitored by splitting off a fraction of the excimer laser onto a calorimeter with a UV-grade fused silica flat. The sampled beam energy is then calibrated against the measured beam energy at the target position. Targets are contained in a four-way glass vacuum chamber evacuated with a turbo-molecular vacuum pump. Experiments were performed in vacuum at a pressure of 3×10^{-4} Torr as monitored by an ionization gauge. The target functioned as the grounded electrode while a copper annulus in front of the target served as the high-voltage electrode. The target was given a hemispherical shape, eliminating electric field enhancement at the edges to ensure the discharge was guided through the plume to the laser ablation spot. Discharge energy was provided by a spark gap switched, three-element, inductor–capacitor pulse forming network (PFN). A 10 Ω resistor placed in parallel with the plasma, in conjunction with a Pearson current transformer, was used to monitor the output voltage. Typical peak discharge parameters were 280–760 A and 1400–3600 V in a 6 μs pulse for charging voltages of 2500–7500 V giving peak instantaneous powers in the 240 kW–1.4 MW range. In this paper the discharges will be referenced by the peak discharge voltage unless otherwise noted.

Optical emission spectroscopy was carried out with a 0.25 m spectrograph containing a 1200 lines per mm grating blazed at 400 nm, coupled to a 1024 diode array gated intensified detector and spectrometer. Temporally resolved spectroscopy used a 0.25 m monochromator with 600 lines per mm gratings, blazed at 300 nm and 600 nm with 150 μm entrance and exit slits. The light was detected at the output with a photomultiplier tube detector. All optics

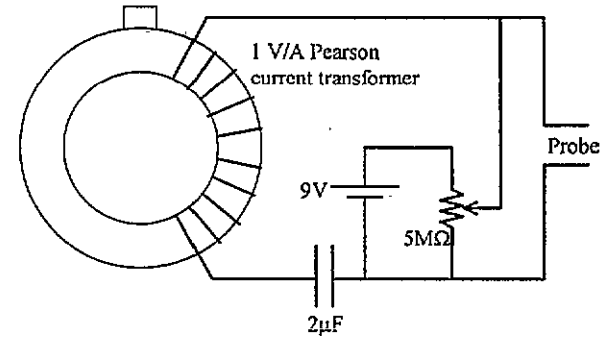

Figure 2. Floating double Langmuir probe electrical circuit schematic.

were made of fused silica, allowing spectra to be obtained down into the ultraviolet. The floating double Langmuir probe consisted of two tungsten wire tips ($L = 0.64$ mm, $D = 0.14$ mm) separated by 1 mm. Bias voltage was supplied with a 9 V battery and potentiometer. The transient signal was measured with ten cable turns through a Pearson current transformer, preserving a fast rise time of 80 ns, while allowing the probe to float as the voltage varied across the discharge gap. Figure 2 shows an electrical schematic of the probe circuit.

3. Results and discussion

Initial experiments with the LAAPDs showed that with the application of the discharge, the usual neutral laser ablation plume was almost completely ionized. This was confirmed by the presence of Al^+ and Al^{2+} ion optical emission with only a small increase in Al neutral optical emission as detected by optical emission spectroscopy [13]. These spectra were time integrated due to systematic constraints. Figure 3 shows a typical time-integrated spectra taken during the discharge. Figure 4 shows the excimer laser as observed on a PIN diode, the discharge voltage on the ring electrode, the discharge plasma current from the ring electrode to the target and the discharge power (magnitude of current multiplied by voltage) as a function of time for a typical PFN charging voltage of 7500 V. In the spectra of figure 3, light was collected from 140 ns to 6 μs after the laser pulse. Without the discharge, optical emission is only observed from the Al neutral transitions at 394.40 nm and 396.15 nm. From the relative emission line intensities of a given species, an electronic temperature can be inferred from an atomic Boltzmann plot [14]. Using Al^+ ion optical emission an electronic temperature of approximately 1 eV is determined, while Al^{2+} optical emission provides an electronic temperature of 3 eV. For the ionic emission lines used, local thermodynamic equilibrium (LTE) is applicable, implying the average electron temperature over the first 6 μs is between 1–3 eV.

With the aid of a monochromator and a photomultiplier tube, the temporal evolution of Al and Al^{2+} optical emission has been examined. The temporal evolution of the Al^+ optical emission was not obtained as no sufficiently strong, isolated Al^+ transition was available. Figure 5 shows the 394.40 nm Al neutral optical emission as a

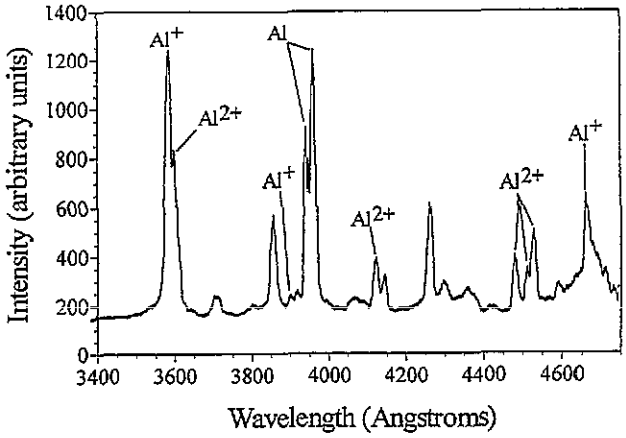

Figure 3. Time-integrated optical emission spectra of 3600 V discharge. Light is collected from 140 ns to 6 μs after the laser pulse. Laser fluence is 10 J cm^{-2}.

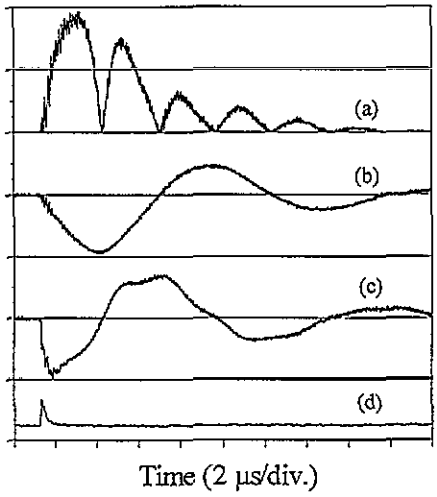

Figure 4. Typical discharge signals from experiment with 7500 V charging voltage: curve a, instantaneous power through discharge plasma (800 kW per division); b, discharge plasma current from ring electrode to target (800 A per division); c, discharge voltage across plasma with respect to grounded target electrode (4 kV per division); and d, PIN diode signal of KrF excimer laser.

function of time with discharge voltage as a parameter, with a laser fluence of 10 J cm^{-2}. Light is sampled from 1 mm in front of the target ablation spot. The signals shown are obtained by subtracting the off-resonance photomultiplier tube signal from the on-resonance signal to eliminate signal contribution due to continuum radiation and recombination light. Each signal was the average of 20 shots with the difference smoothed using a 6-bit running average to eliminate high-frequency noise. The excimer laser as detected by a PIN photodiode is also shown for a time reference in figure 5, curve f. Figure 5 curve a shows the optical emission from laser ablation only (no discharge present). The signal contains a component with a fast decay followed by a component with a long decay due to slower moving particles. With the application of 1400 V as shown in figure 5 curve b, Al neutral optical emission is now observed at much later times than with no discharge, indicating excited aluminium atoms are still present as late as 10 μs. As the discharge voltage is increased, the Al

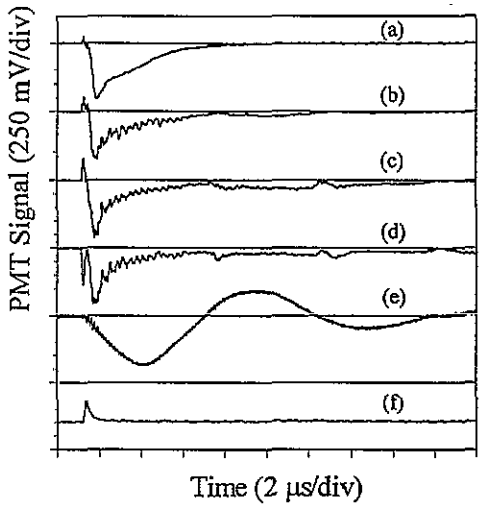

Figure 5. Time-resolved 394.40 nm Al neutral optical emission signal with a laser fluence of 10 J cm^{-2}. Curve a, laser ablation only; b, laser ablation with 1400 V discharge; c, laser ablation with 2400 V discharge; d, laser ablation with 3600 V discharge; e, discharge plasma current from ring electrode to target; f, PIN diode signal of KrF excimer laser.

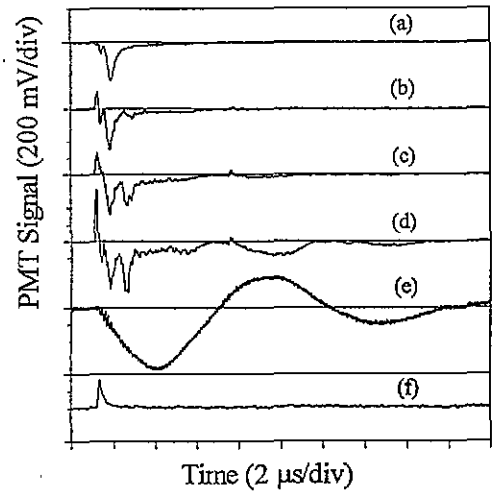

Figure 6. Time-resolved 452.92 nm Al^{2+} ion optical emission signal with a laser fluence of 10 J cm^{-2}. Curve a, laser ablation only; b, laser ablation with 1400 V discharge; c, laser ablation with 2400 V discharge; d, laser ablation with 3600 V discharge; e, discharge plasma current from ring electrode to target; f, PIN diode signal of KrF excimer laser.

neutral optical emission appears to peak at around 2400 V (figure 5, curve c) with a reduction in emission at 3600 V (figure 5, curve d) as compared to 2400 V. This implies the higher voltage leads to more ionization and hence less neutral excitation and optical emission. Comparing the emission intensity from figure 5 curves b–d to the plasma current (curve e), it can be seen that the optical emission intensity closely follows the current through the plasma.

Figure 6 shows the optical emission from the 452.92 nm Al^{2+} ion transition as a function of time for different discharge voltages with a laser fluence of 10 J cm^{-2}. The traces shown in the figure are again the result of subtracting the off-resonance PM tube signal from the on-resonance signal with each signal a 20 shot average and the difference

smoothed with a 6-bit running average. Observe in figure 6 curve a, which shows the Al^{2+} ion emission as a function of time with laser ablation only, there is a small amount of Al^{2+} ion emission at very early times. While spectra taken with a spectrograph also confirm there is Al^{2+} ion optical emission with laser ablation alone, it only occurs for times less than approximately 150 ns. Therefore, the emission signal in figure 6 curve a immediately after the laser pulse is probably due to a slight difference in the spectral response of the detector and monochromator at the off- and on-resonance wavelengths, since it represents the difference of two large signals. Furthermore, the signal present with laser ablation only is also present in the other three traces including the discharge. Note that this was not important for figure 5, as the on-resonance signal was much larger than the off-resonance signal. Comparison of the absolute signal strengths cannot be made between figures 5 and 6, as the PMT voltage was increased in figure 6 to improve the signal-to-noise ratio. The positive signal (also in figure 5) is due to noise from the breakdown of the spark gap switch and occurs before the ablation laser strikes the target. (The high impedance of the PMT makes it very sensitive to noise.)

Figure 6 curve b shows a small increase in the Al^{2+} optical emission with the 1400 V discharge present. Increasing the voltage to 2400 V yields slightly more Al^{2+} emission, but the most noticeable feature of figure 6 curve c is the large burst of emission approximately 2 μs after the excimer laser pulse and discharge initiation. Increasing the voltage to 3600 V, as in figure 6 curve d, further increases the intensity of the Al^{2+} optical emission burst, but now results in a large increase in the emission at later times. As the discharge voltage and current are increased, the temperature of the plasma is increased, which results in higher charge states being created. This also agrees with figure 5, which shows reduced Al neutral optical emission as the voltage is increased.

It can be observed from figure 6 curve e that the evolution of the Al^{2+} optical emission intensity follows the plasma current. The large burst of Al^{2+} emission 2 μs after the laser pulse coincides with the first maximum in the power (see figure 4 curve a). This is also the first time the neutral plume is broken down and the discharge created, with the density of ablated matter highest. When the current goes to zero (the second time at ~ 6 μs), the Al^{2+} optical emission ceases until the discharge is re-initiated due to the still appreciable voltage on the electrode.

To measure the ion density present in the discharge, a floating double Langmuir probe was used. (This was a necessity, as the discharge voltage of the plasma changed as a function of time.) For each data point at a given bias voltage, ten shots were averaged to reduce effects of noise. The probe was positioned approximately 1 mm in front of the laser ablation spot, such that the probe tip was parallel to the target surface. Figure 7 shows the probe current as a function of the bias voltage. The asymmetry in the signal is due to the probe tip separation being comparable to the laser spot size and a slight offset of the probe from the centre of the laser spot. For bias voltages greater than 5 V, the current rapidly increases, signifying breakdown

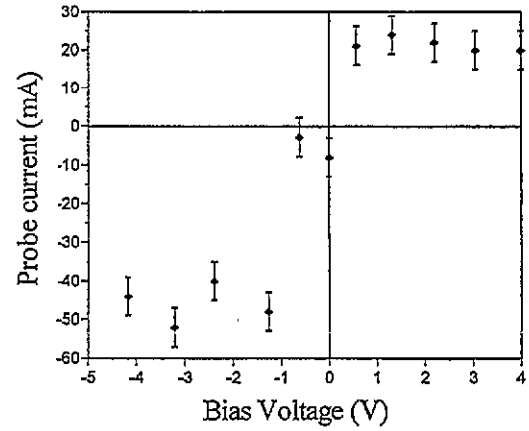

Figure 7. Floating double Langmuir probe current data as a function of bias voltage. Data points represent the average current value over the second lobe of the discharge current. Laser fluence is 10 J cm^{-2} with 5000 V PFN charging voltage.

between the probe tips. The charging voltage was 5000 V (peak discharge voltage 2400 V) and each point represents the time-averaged current over the second current lobe (6–12 μs), as the signal at earlier times contained too much noise to extract any reliable information. From the theory of double Langmuir probes [15], the experimental data of figure 7 imply an electron temperature of approximately 1 eV and a time-averaged ion density of approximately 5×10^{14} cm^{-3} during the second current lobe (6–12 μs). As the plume density decreases with time, the ion density is likely to be higher during the first 6 μs.

To predict the ionization fractions in the aluminium plasma as a function of electron temperature, a simple local thermodynamic equilibrium (LTE) model is used. This model uses the Saha equation, conservation of particles and conservation of charge. By assuming a value for the electron density, the fraction of each ionization state, as a function of electron temperature, may be determined. This is shown in figure 8, where an electron density of 1×10^{15} cm^{-3} has been assumed to be consistent with previous laser deflection measurements [6], VUV spectroscopy of aluminium KrF excimer laser ablation [16], and the Langmuir probe ion density measurement. The figure shows that for equal fractions of Al^{+} and Al^{2+} ions, the model predicts an electron temperature of 1.2 eV in reasonable agreement with the spectroscopic measurement using Al^{+} ion optical emission and the Langmuir probe measurement. However, it should be noted that these values differ from the electron temperature of 3 eV inferred from Al^{2+} ion optical emission. A possible explanation is that the electron distribution function is not exactly Maxwellian, but may have a high-energy tail. Since the Al^{+} optical emission comes from 10–16 eV above the ground state, while the Al^{2+} optical emission comes from transitions 18–23 eV above the ground state, the Al^{+} emission could be excited by the Maxwellian part of the distribution, while the Al^{2+} emission could be excited by the high-energy tail, thus explaining the higher inferred electron temperature. Furthermore, since the electron temperature is changing with time, the Al^{2+} ions may be formed at a hotter stage

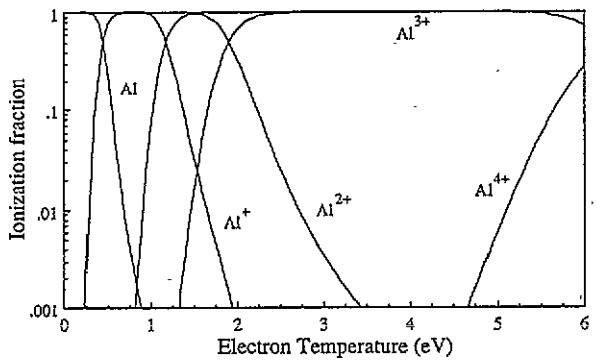

Figure 8. LTE model results showing ionization fraction as a function of electron temperature for Al plasma assuming an electron density of 10^{15} cm^{-3}.

during the discharge than the Al^+ ions, resulting in the difference in inferred electron temperatures taken from the time-integrated emission spectra.

In summary, spectroscopic measurements indicate an electron temperature of 1 eV using relative emission intensities of Al^+ ions, while 3 eV is inferred using Al^{2+} ion emission. As the spectra were time integrated, these are averages over the first current lobe, implying an electron temperature between 1–3 eV. A simple LTE model employing the Saha equation prediction of the ionization fraction as a function of electron temperature indicates a temperature of 1.2 eV for approximately equal Al^+ and Al^{2+} ion fractions present in the discharge, as implied through the emission spectra. Hence, the probe measurement of 1 eV for the electron temperature between 6 and 12 μs is consistent with previous results. With the resonant-holographic-interferometry (RHI) diagnostic, the total number of ablated aluminium neutral particles has been previously measured to be approximately 3×10^{14} [5], however in those experiments the fluence was ~ 4 J cm^{-2}. Since the plume volume was slightly smaller than 1 cm^3, the Langmuir probe measurement of 5×10^{14} cm^{-3} for the ion density (with a fluence of 10 J cm^{-2}) is reasonable.

Future work will focus on applying resonant dye laser diagnostics to the discharge plasma, thus extending their use to ion species for the measurement of two-dimensional line density profiles.

Acknowledgments

This research was supported by National Science Foundation Grant CTS-9108971. JSL and HLS acknowledge the National Science Foundation for Graduate Fellowships. The authors acknowledge the technical assistance of R Spears and C H Ching.

References

[1] Krebs H and Bremert O 1993 *Appl. Phys. Lett.* **62** 2341
[2] Balla A K, Salamanca-Riba L, Doll G L, Taylor C A and Clarke R 1992 *J. Mater. Res.* **7** 1618
[3] Geohegan D B 1993 *MRS Proc.* **285** 27
[4] Lindley R A, Gilgenbach R M and Ching C H 1993 *Appl. Phys. Lett.* **63** 888
[5] Lindley R A, Gilgenbach R M, Ching C H, Lash J S and Doll G 1994 *J. Appl. Phys.* **76** 5457
[6] Gilgenbach R M, Ching C H, Lash J S and Lindley R A 1994 *Phys. Plasmas* **1** 1619
[7] Dreyfus R W 1991 *J. Appl. Phys.* **69** 1721
[8] Dimberger L, Dyer P E, Farrar S R and Key P H 1993 *Proc. Second Int. Conf. on Laser Ablation* (New York: AIP)
[9] Geohegan D B 1993 *Appl. Phys. Lett.* **62** 1463
[10] Krishnaswamy J, Rengan A, Narayan J, Vedam K and McHargue C J 1989 *Appl. Phys. Lett.* **54** 2455
[11] Ying Q Y, Shaw D T and Kwok H S 1988 *Appl. Phys. Lett.* **53** 1762
[12] Collins C B, Davanloo F, Jeungeman E M, Osborn W S and Jander D R 1989 *Appl. Phys. Lett.* **54** 216
[13] Lash J S, Gilgenbach R M and Ching C H 1994 *Appl. Phys. Lett.* **65** 531
[14] Marr G V 1968 *Plasma Spectroscopy* (New York: Elsevier)
[15] Johnson E O and Malter L 1950 *Phys. Rev.* **80** 58
[16] Mehlman G, Chrisey D B, Burkhalter P G and Horwitz J S 1993 *J. Appl. Phys.* 74 53